Ultrafast light-induced charge pair formation dynamics in poly[3-(2′-methoxy-5′octylphenyl)thiophene]

Yuri Zaushitsyn,[1] Vidmantas Gulbinas,[2] Donatas Zigmantas,[1] Fengling Zhang,[3] Olle Inganäs,[3] Villy Sundström,[1] and Arkady Yartsev[1,*]

[1]*Department of Chemical Physics, Lund University, P.O. Box 124, SE-22100 Lund, Sweden*

[2]*Institute of Physics, Savanoriu 231, LT-02300, Vilnius, Lithuania*

[3]*Department of Physics (IFM), Linköping University, SE-58183 Linköping, Sweden*

(Received 10 July 2003; revised manuscript received 15 March 2004; published 5 August 2004)

Charge pair photogeneration was investigated by ultrafast absorption spectroscopy for different excitation photon energies in poly[3-(2′-methoxy-5′octylphenyl)thiophene] (POMeOPT) film with and without an external electric field. Electric field-assisted charge pair photogeneration in POMeOPT occurs from vibrationally relaxed singlet excitons during their entire lifetime and charge pair formation takes place in this manner even in the absence of an external electric field. From our data there are no indications of hot exciton dissociation to charge pairs even when a large amount of excess energy is supplied to the excitons. To explain these observations we present a model with energy transfer to low-barrier dissociation sites as a key feature.

DOI: 10.1103/PhysRevB.70.075202 PACS number(s): 78.47.+p, 42.65.Re, 78.55.Kz, 78.66.Qn

I. INTRODUCTION

Conjugated polymers could be used in both light emitting devices (LED) and solar cell applications. Organic LED technology has reached great progress in the last decade, and is still rapidly growing. There are already commercially available organic polymer devices and displays, which could have a thickness less than 1 mm and be built on flexible substrates. At the same time, in solar cell applications the maximum light-to-current efficiency is far from the theoretical prediction for conjugated polymers, leaving room for much future work before cheap and effective organic solar cells can be realized. An important step in this work is to reach an understanding of the processes, that control the light-to-charge conversion. The sequence of events that occurs in this process is poorly understood. Upon optical absorption an excited state (exciton, sometimes labeled a neutral bi-polaron) is formed and as a sequel to that generation of charge carriers may occur. In what follows we will use the notion "charge pair" to describe the electron-hole pair formed by light absorption. Other similar concepts found in the literature are, polaron pair or simply polaron(s), but since our measurement technique is not sensitive to the interaction between the charges, i.e., whether the charges are bound or not, we will use the term "charge pair."

Several different models of charge generation have been proposed, even for the same polymers, by different research groups. There are basically two main pictures of charge generation in conjugated polymers: direct photogeneration of free charges via optical excitation[1,2] and formation of charge pairs from neutral singlet excitons.[3–14] While most of the results in the literature support the latter picture, there is no agreement regarding model, time scale and mechanism of singlet exciton splitting to the charge pair. Kersting *et al.* investigated the dynamics of field-induced fluorescence quenching in a blend system of 20% poly(phenylphenylenvinylene) and 80% polycarbonate.[3] They observed that the main quenching occurs within several ps after excitation and continues on a time scale of several hundred ps. They proposed that the quenching dynamics are related to the interplay of the exciton breaking and spectral relaxation of excitons within the inhomogeneously broadened density of states. Based on the temperature, photon energy and field dependence of the photocarrier yield, observed by Barth *et al.* in polyphenylenevinylene (PPV) (Ref. 4) and in methyl-substituted ladder-type poly-para-phenylene (MeLPPP),[5] Arkhipov and co-workers developed a theory of field assisted on-chain hot exciton dissociation.[6,7] They proposed that charge separation occurs on the subpicosecond time scale, assisted by the excess vibrational energy. From observation of the rapid onset of stimulated emission quenching and transient absorption due to charged species in MeLPPP, with an external applied electric field and high intensity ($1.2\ \mathrm{mJ/cm^2}$) excitation by photons with low excess energy ($\sim$0.5 eV), Graupner *et al.*[8] proposed that these processes occur on two separate time scales. Excitons turn into polarons at "dissociation sites" that are found during exciton interchain thermalization on the time scale of 2–3 ps. Slow and less efficient charge pair generation is explained by the diffusion of excitons approaching the localization edge. Our previous investigation of field-assisted charge pair and exciton dynamics in MeLPPP shows that (1) under excitation with low excess energy ($\sim$0.5 eV) and low excitation intensity ($14\ \mu\mathrm{J/cm^2}$) the dissociation of excitons into electron-hole pairs occurs from the vibrationally relaxed excited state throughout its lifetime;[9] (2) after excitation to higher exciton states ($\sim$2 eV excess energy), two additional ultrafast generation steps appear, charge pair generation during the relaxation of highly excited states (instantaneous or faster than 200 fs) and field assisted breaking of the hot S_1 state during a time interval of $\sim$2 ps.[10] Recent photocurrent and photoluminescence experiments on MeLPPP by Muller *et al.*,[11] showed that excitons ($\sim$0.5 eV excess energy) can relax in two ways: 90% form "cold," i.e., vibrationally relaxed excitons that dissociate to charge carriers throughout their lifetime and 10% instantaneously generate intrachain charge

pairs. Double excitation to high-lying excited states increases photoionization efficiency by about two orders of magnitude in a polyfluorene polymer (PIFTO), as was shown by Silva *et al.*[12] They proposed a model of charge generation from high-lying excited states, which can be reached by double excitation during the laser pulse or by singlet–singlet exciton annihilation. Also in Ref. 13, Denton *et al.* demonstrate the importance of exciton annihilation for charge generation in PPV as every second annihilation process ends up in formation of a charge pair at their experimental conditions.

Most of the work cited above was performed on a few polymers (basically MeLPPP, PPV, and polyfluorene families). Thus, from these results it is not possible to judge whether the mechanism of charge generation is common to all conjugated polymers, or whether it is material specific. We decided to address this problem by investigating a different type of polymer, a polythiophene polymer. Results available in the literature[14,15] suggest that this type of polymer exhibits light induced charge formation also in the absence of an applied external electric field. Thus, low photon energy optical excitation forms charge pairs in poly(3-(4-octylphenyl)-2,2′-bithiophene (PTOPT) (Ref. 14) and poly (3-butyl-thiophene) (P3BT),[15] with a characteristic photoinduced absorption (PA) in the 1.2 eV–2.2 eV spectral region. For polythiophenes, triplet states are known to absorb in the same spectral region, but photoinduced absorption detected magnetic resonance (PADMR) spectroscopy[16] shows that $\sim 2/3$ of the signal in P3BT at 1.3–2.0 eV is due to photoinduced charge pair absorption.[15] Similar structure, steady-state absorption and fluorescence spectra of PTOPT, P3BT, and POMeOPT suggest that these polythiophenes could have similar spectroscopic properties.

We have studied POMeOPT as a representative of the polythiophene family and measured ultrafast electric field assisted dynamics of excitons and charge pairs at two excitation photon energies and different excitation intensities. The dependence of charge pair formation on applied electric field strength was studied as well. Our results show that the charge photogeneration in POMeOPT is substantially different from that in MeLPPP.[9,10] It is best characterized as a low-barrier process occurring at a low concentration of dissociation sites reached by energy migration and direct excitation. We present a quantitative model to describe the charge generation.

II. EXPERIMENT

POMeOPT was synthesized as described in Ref. 17. The polymer films were deposited on indium-tin oxide (ITO) covered glass by spin coating from chloroform solution, to a film thickness of about 100 nm. Thin aluminum electrodes were evaporated on top of the polymer in a vacuum chamber. As these polymer films are oxygen sensitive and destroyed in several days in contact with air, the structure was sealed from air by gluing a thin cover glass using a Variant polymer as glue. Absorption and emission spectra of this device were in accordance with previous reports[17] and did not change during several months. The pump-probe absorption spectrometer was described elsewhere.[14] The sample was excited by 120 fs pulses with 5 kHz repetition rate at 500 nm (2.5 eV) and 400 nm (3.1 eV), i.e., about 0.5 eV and 1.1 eV above the polymer absorption edge. A white-light continuum was generated in a 5 mm sapphire window from the Ti:Sa fundamental at 800 nm, or from 1400 nm pulses generated by an OPA (TOPAS). With this probe light we could monitor the 1.15–2.45 eV spectral region. At 1240 nm (1 eV) and 800 nm (1.55 eV) the probe was taken directly from the TOPAS or from the Ti:Sa amplifier. Excitation and probing were performed through the glass support, and the probe beam was monitored after its reflection from the aluminum electrode. The reference beam, which was taken from the probe beam before focusing into the sample, passed through the film with no external electric field and no light excitation and was monitored after reflection from another aluminum electrode.

To probe the effect of an applied electric field, 0–22 V and 10 μs long field pulses were applied during every second optical pulse. To avoid charge carrier injection we used reverse bias, i.e., the aluminum electrode was positively biased. As the resistance of our device was more than 30 MΩ at maximum voltage, the concentration of injected charges from electrodes was less than 10^{14} cm^{-3}, negligible in comparison to the concentration of excitons and charge pairs (10^{16}–10^{20} cm^{-3}) created by the excitation light. The excitation-induced difference in optical density of the sample, with and without external electric field was measured as

$$EDA = A^F - A = \lg\left(\frac{I_p^F}{I_r^F}\right) - \lg\left(\frac{I_p}{I_r}\right), \tag{1}$$

where I_p and I_r are the probe and reference intensities without the external electric field, I_p^F is the probe intensity with the electric field, I_r^F is the reference intensity measured simultaneously with I_p^F. The pump pulse was applied for every probe pulse. The delay time between the probe and pump pulses was varied from −20 ps to 730 ps. Pump-probe experiments described below were performed at the magic angle (54.7°) between pump and probe polarizations.

Anisotropy decay measurements were performed using a femtosecond transient absorption spectrometer with 20–30 fs light pulses, described elsewhere.[18] The excitation wavelength was 500 nm (2.5 eV) with a spectral width of 17 nm (FWHM) and the probe wavelength was 570 nm (2.2 eV) with 32 nm width. The intensity of pump pulses was ~ 20 μJ/cm^2. Differential absorption and transient anisotropy measurements were performed by setting a 45° angle between the pump and probe pulse polarizations, detecting the probe components parallel, $\Delta A_{\parallel}$, and perpendicular, $\Delta A_{\perp}$, to the pump polarization simultaneously but independently. Because $\Delta A_{\parallel}$ and $\Delta A_{\perp}$ were measured using components of the same initial pulses, carrying the same fluctuations, the anisotropy $r(t) = (\Delta A_{\parallel} - \Delta A_{\perp})/(\Delta A_{\parallel} + 2\Delta A_{\perp})$ was measured with a very high signal to noise ratio. Anisotropy experiments with lower time resolution were performed using fluorescence streak camera measurements, described elsewhere.[19] In these experiments the sample was excited at 400 nm (3.1 eV) with the same excitation intensity

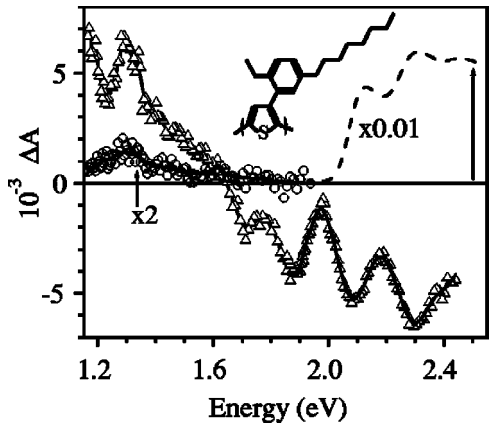

FIG. 1. Differential absorption spectrum of POMeOPT at 1 ps (triangles) and 400 ps (circles) after low photon energy and low intensity excitation. Dashed line, absorption spectrum. Insert, POMeOPT structure.

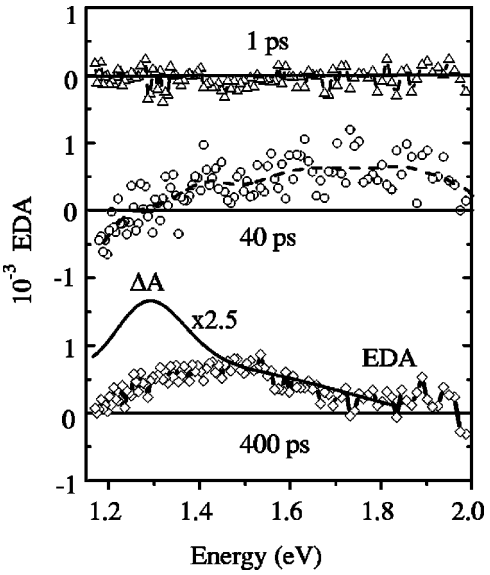

FIG. 2. Stark shift subtracted electroinduced differential absorption (EDA) spectra at different time delays after 75 $\mu J/cm^2$ excitation under $\sim 2\times 10^6$ V/cm external electric field. Solid line is ΔA spectrum multiplied by a factor of 2.5 at 400 ps after 30 $\mu J/cm^2$ excitation.

as in transient absorption anisotropy experiments. Fluorescence kinetics with parallel and perpendicular polarizations to the pump were measured with 10 ps time resolution and then anisotropy was calculated.

III. RESULTS AND DISCUSSION

A. Spectral characteristics of charge pairs, singlet and triplet excitons

POMeOPT (structure is shown in the inset of Fig. 1) has a broad absorption spectrum, starting at 2 eV (the red part of it is plotted in Fig. 1). The differential absorption (ΔA) spectra of POMeOPT film at 1 and 400 ps after low photon energy (2.5 eV) and low intensity (~ 30 $\mu J/cm^2$) excitation are shown in Fig. 1. This photon energy is 0.5 eV above the red onset of the absorption spectrum and therefore corresponds to a modest excess energy. A negative ΔA signal corresponds to absorption photobleaching and stimulated emission (SE) of singlet excitons. As mentioned above, the transient spectrum of a polythiophene could have contributions from charge pairs and triplet excitons in the 1.2 eV–2.2 eV spectral region. A positive signal could therefore have three contributions–photoinduced absorption (PA) of singlet excitons, charge pairs and triplet excitons. Figure 1 shows that even at long times after excitation, PA does not vanish. Data in Fig. 3 shows that the singlet exciton concentration at 400 ps is more than 100 times smaller than the initial exciton concentration. From this we conclude that the differential absorption signal at 400 ps has contributions from long-lived charge pairs and triplet excitons.

Electroinduced differential absorption (EDA) spectra were measured in the 1.17–2.45 eV region after 2.5 eV photon energy and ~ 75 $\mu J/cm^2$ light intensity excitation in POMeOPT film in the presence of an $\sim 2\times 10^6$ V/cm external electric field. The Stark shift signal at energies higher then 2 eV is 10–20 times more intense than that related to charge pair PA and quenching of the exciton SE, and therefore this spectral region will not be considered in this work. In the rest of the spectrum the Stark shift signal measured at negative delay time was subtracted from the EDA spectra. The EDA spectra at 1, 40, and 400 ps after excitation, with the Stark shift contribution subtracted, are plotted in Fig 2. The subtraction does not fully eliminate the Stark shift influence above 1.9 eV because it could be time dependent.[20] In the rest of the spectrum a positive EDA signal corresponds to electroinduced charge pair absorption and to exciton SE quenching. The negative signal observed at <1.27 eV is caused by quenching of exciton PA. There is a small negative triplet signal contribution to the EDA, due to decrease of singlet exciton concentration. An estimate shows that the maximum value of the triplet signal is 0.0001, which is less than the noise level of the spectral measurements. Therefore, we neglect the triplet exciton contribution to the EDA spectra. During the first picoseconds the EDA signal is very weak, because of a low field induced charge pair concentration, and/or cancellation of the charge pair signal by electroinduced exciton absorption quenching. On a longer time scale (40 ps), a positive signal appears due to quenching of SE (~ 1.65–2.0 eV) and photoinduced charge pair absorption. In comparison with the 400 ps EDA spectrum, the 40 ps spectrum has higher signal amplitude at energies >1.65 eV and lower, even negative signal, at energies <1.55 eV. This difference is caused by the contributions to the EDA signal from the field induced exciton quenching, SE (>1.65 eV, positive signal) and PA (<1.65 eV, negative signal). At 400 ps, only electroinduced absorption of charge pairs and the time-dependent Stark shift contribute to the EDA. Photoinduced charge pair absorption has a broad spectrum with maximum at 1.45 eV and a width at half-maximum of 0.4 eV. For comparison, the EDA and ΔA spectra at 400 ps are plotted in Fig. 2. At energies higher than 1.5 eV they coincide, but the ΔA spectrum has an additional band at ~ 1.3 eV. We attribute this band to triplet exciton PA. The

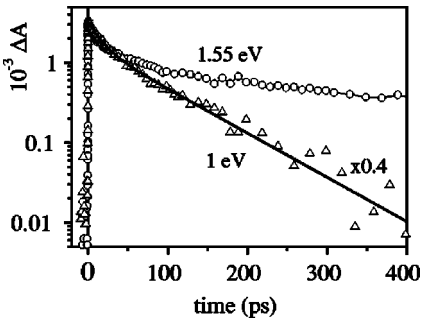

FIG. 3. Normalized differential absorption kinetics at the probe energies 1.55 eV (circles) and 1.0 eV (triangles, solid line, the two exponential fit). The 1.0 eV kinetics is multiplied by a factor of 0.4.

transient absorption spectrum in Fig. 1 shows an isobestic point at ~1.6 eV. The contribution to the EDA spectra from the singlet exciton quenching is therefore relatively weak in this spectral region. We have chosen to probe the appearance of the charge pairs at 1.55 eV, and corrected the measured signal from the small contribution of exciton signal that is still present at this probe energy.

We now identify a spectral region for monitoring singlet excitons. To this end we measured the differential absorption kinetics at 1.0 eV, with 2.5 eV photon energy and ~75 μJ/cm^2 light intensity excitation (Fig 3). The kinetic curve returns to the base line after ~300 ps, showing that triplets or charge pairs do not contribute to the ΔA signal in this spectral region, since their lifetimes are much longer.[14,15] The bi-exponential fit to this curve yields two lifetimes, 14 and 85 ps. The first time component is due to energy transfer, singlet exciton-exciton annihilation and charge pair formation. The second decay component represents the singlet exciton lifetime in POMeOPT. Thus, we conclude that singlet exciton decay can be monitored at 1 eV, free of contamination from other species.

Figure 3 also displays the ΔA kinetics measured at 1.55 eV under the same excitation conditions as the 1.0 eV kinetics. The dynamics at 1.55 eV are more complex—there are two main contributions; singlet exciton dynamics (energy transfer, annihilation and intrinsic decay) and charge pair formation and decay. The key difference between the kinetics at these two probe energies is related to the ~0.45±0.05 ns component, which corresponds to long-lived charge pairs. A single exponential fit on a time scale longer than 200 ps gives no evidence for other long time components in the differential absorption dynamics. The absence of an offset in the ΔA kinetics, the similar decay of charge pair EDA signal at this wavelength (see below) and the fact that the EDA and ΔA spectra at long times are identical near 1.55 eV, show that the triplet contribution to the ΔA signal at 1.55 eV is insignificant. This in its turn implies that the signal amplitude at 1.55 eV in the ΔA spectrum on a long time scale (400 ps) (Fig. 1) must be due to charge pairs, and consequently charge pairs are formed also in the absence of an external electric field.

B. Electroinduced charge pair generation

EDA dynamics measured at the probe energies 1.0 and 1.55 eV, after 2.5 eV excitation (~75 μJ/cm^2 intensity), in the presence of $\sim 2\times 10^6$ V/cm external electric field, are displayed in Fig. 4(a). The EDA at 1.0 eV represents electroassisted quenching of excitons and at 1.55 eV charge pair dynamics. As was discussed above, the signal at 1.55 eV also contains a small contribution from singlet excitons. In order to obtain the pure charge pair response the exciton contribution has to be subtracted from the measured response:

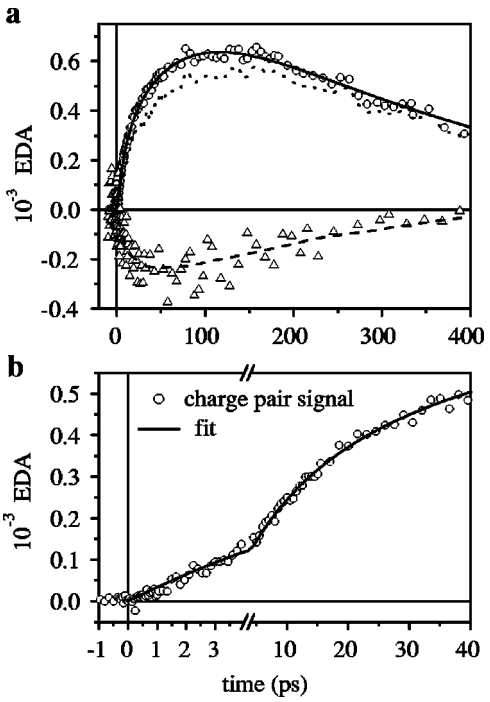

FIG. 4. (a) EDA (exciton) dynamics probed at 1.0 eV, after 2.5 eV and 75 μJ/cm^2 excitation (triangles and dashed line); non-subtracted charge pair EDA (dotted line) and exciton subtracted EDA [circles, solid line, fit by formula (3)] probed at 1.55 eV. (b) Charge pair EDA dynamics probed at 1.55 eV on a short time scale; solid line, fit by formula (3).

$$n_{cp}^{F}(t) l \sigma_{cp}^{(1.55)} = \mathrm{EDA}_{cp}^{(1.55)} = \mathrm{EDA}^{(1.55)} - \frac{\sigma_e^{(1.55)}}{\sigma_e^{(1.0)}} \mathrm{EDA}^{(1.0)}. \tag{2}$$

We determine the exciton cross section ratio $\sigma_e^{(1.55)}/\sigma_e^{(1.0)} = 0.4$ from the ratio of $\Delta A_{\max}$ of the differential absorption kinetics in Fig. 3. If all charge pairs were formed directly after photoexcitation, the cross section ratio obtained in this manner would be up to 20% lower, but would not change qualitatively the following considerations. The corrected charge pair EDA response (open circle symbols in Fig. 4) rises from zero and can be fitted to a three-exponential law (two rise components and one decay):

$$\mathrm{EDA}_{CP}^{(1.55)} = B(e^{-t/t_3} - e^{-t/t_1}) + C(e^{-t/t_3} - e^{-t/t_2}). \tag{3}$$

A fit gives $B=(0.24\pm0.02)\times10^{-3}$ for the fast rise component, $t_1=9.6\pm0.9$ ps, and $C=(0.93\pm0.04)\times10^{-3}$ for the slow rise component, $t_2=71\pm5$ ps; the decay time $t_3=320\pm20$ ps is comparable with the 450 ± 50 ps time constant in the field-free kinetics. As can be seen from Fig. 4(b), there is no

instantaneous charge pair formation—the appearance of the charge pairs is well described by the 9.6 and 71 ps rise time components and formation proceeds throughout the singlet exciton lifetime. This characterization in terms of time constants for the charge pair formation does not provide physical insight into the charge generation mechanism. The model presented below yields this knowledge and the fitting to the experimental result in Fig. 4 is generated with this model (see below).

The charge pair yield φ can be estimated from EDA and ΔA kinetics at 1.0 eV. In the molecular approach, the number of formed charge pairs is equal to the number of broken excitons, i.e., φ is the ratio between the number of broken excitons and the number of initially excited excitons. The additional yield of electroassisted charge pair formation can be estimated as

$$\varphi_e = \frac{\int_0^\infty \mathrm{EDA}^{(1.0)}\, dt}{\int_0^\infty \Delta A^{(1.0)}\, dt}. \tag{4}$$

From the data of Fig. 3 and 4 we obtained $\varphi_e = 13\%$. It will be shown later that the charge pair yield without external field is equal to the additional charge pair formation yield with ~ 2 MV/cm external electric field, $\varphi = \varphi_e = 13\%$.

The charge pair formation dependence on excitation photon energy was studied through increasing excitation photon energy from 2.5 to 3.1 eV. In order to excite the same number of singlet excitons at the two energies, an excitation density of 180 μJ/cm^2 was chosen at 3.1 eV. The differential absorption and EDA dynamics, for both excitation energies, monitored at 1.55 eV are shown in Fig. 5. The differential absorption dynamics are identical within experimental accuracy for the both excitation conditions, showing that for both excitations the same number of charge pairs are formed. The EDA dynamics are also identical within experimental accuracy [Fig. 5(b)]. At both excitation energies the dynamics start from the zero level and rise slowly. There is no instantaneous rise component of the EDA dynamics, indicating that an increase of the excess energy by more than a factor of 2 does not lead to very fast hot exciton dissociation to charge pairs. Since no external electric field induced ultrafast charge formation from hot unrelaxed excitons is observed, it appears reasonable to assume that there is also no hot exciton dissociation in the absence of external electric field. The reason is that an external electric field should increase the probability of exciton dissociation.[3–10] Thus, the charge formation is governed by the same mechanism at both excitation energies.

C. Field dependence of charge pair formation in POMeOPT

To study the exciton dissociation mechanism in more detail, the voltage dependence of charge pair generation efficiency was investigated by measuring the EDA at 1.55 eV at 100 ps delay after excitation (Fig. 6). The EDA signal starts

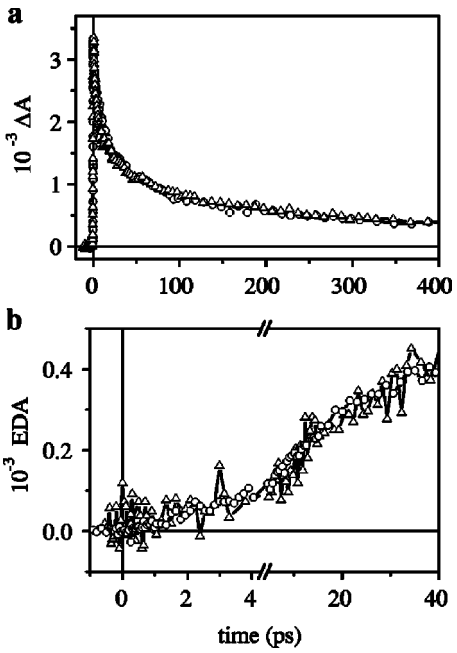

FIG. 5. (a) Differential absorption and (b) EDA dynamics probed at 1.55 eV after 2.5 eV (circles) and 3.1 eV (triangles) excitation with the same number of initially formed excitons.

to grow at very low voltage and increases nonlinearly. In contrast to MeLPPP,[9] a discernable amount of charge pairs are formed even at a fifth of the maximum voltage used ($\sim$0.4 MV/cm). If we assume a similar charge separation distance (6–7 Å) as for MeLPPP,[20] a field of $\sim$0.4 MV/cm corresponds to a field induced reduction of the dissociation barrier by $\sim$26 meV ($\approx kT$ at room temperature). This quite small barrier reduction, resulting in a measurable concentration of charge pairs, means that the charge carrier formation is nearly barrierless or has a low barrier comparable with kT. The voltage dependence of the EDA signal in Fig. 6 can be fitted to a parabolic law:

$$\mathrm{EDA} = aE^2 \tag{5}$$

with $a = 1.17 \times 10^{-4}$ (cm/MV)^2. The parabolic dependence is typical for barrierless electron donor–acceptor transfer.[21] This is further support to a low-barrier electric field-assisted charge pair generation in POMeOPT. A low-barrier process might suggest a high yield of charge generation. The fact that

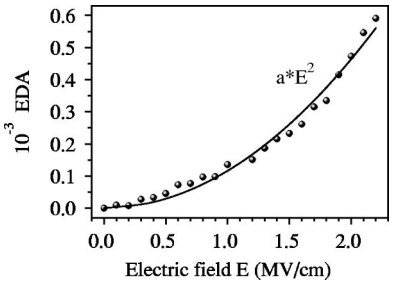

FIG. 6. Voltage dependence of charge pair EDA (circles). Solid line is a parabolic fit: EDA$= a * E^2$, with $a = 1.17 \times 10^{-4}$ (MV/cm)$^{-2}$.

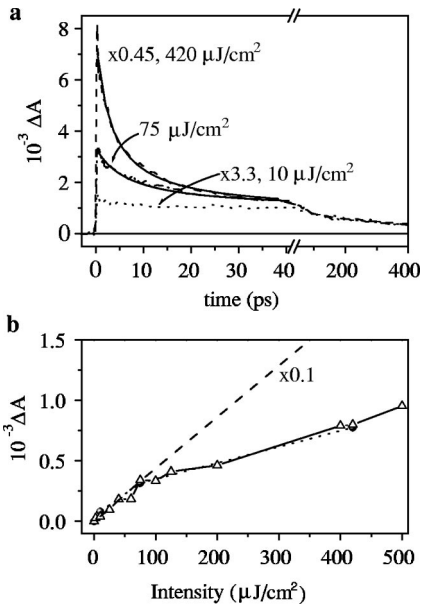

FIG. 7. (a) ΔA kinetics measured at 1.55 eV and normalized on a 200–400 ps time scale. Excitation intensities, 10 μJ/cm^2 (dotted line), 75 μJ/cm^2 (dashed–dotted line), and 420 μJ/cm^2 (dashed line). Solid lines are fits by formula (7). (b) Initial exciton concentration (dashed line), normalized total photoluminescence (dotted line, circles), and charge pair signal (solid line, triangles).

we observe a yield of only 13% for POMeOPT in the absence of external electric field suggests that not every exciton participates in charge formation. This will be further discussed in the model below.

D. Charge pair formation at high excitation intensity

We investigated the charge pair formation as a function of excitation light intensity, to examine whether the formation dynamics is intensity dependent. From these studies we could also conclude that direct optical excitation of charge pairs is not a major mechanism for the charge pair formation. We start by considering the field-free dynamics. Differential absorption kinetics were probed at 1.55 eV (2.5 eV excitation) for 10, 75, and 420 μJ/cm^2 excitation intensities. Figure 7(a) shows the ΔA kinetics at the three intensities, normalized on a long time scale (200–400 ps) to the kinetics at 75 μJ/cm^2 intensity. All three kinetic curves have the same long-lived decay component of 0.45 ns attributable to the charge pair decay. The dynamics at 75 and 420 μJ/cm^2 have in addition fast nonexponential components caused by singlet-singlet exciton annihilation. The fact that the annihilation related decay is much faster than the singlet exciton lifetime shows that there are multiple excitations within a domain of interacting excitons, and that excitons at these intensities may undergo multiple annihilation events until the exciton density is reduced below the annihilation threshold. The annihilation can be described by an effective rate β,[13] which is time independent. The singlet exciton concentration $n(t)$ in that case can be found from the following kinetic equation:

$$\begin{cases} \dfrac{dn(t)}{dt} = -kn(t) - \beta n^2(t), \\ n(t)|_{t=0} = n_0, \end{cases} \tag{6}$$

as

$$n(t) = \frac{n_0 e^{-kt}}{1 + n_0 \beta k^{-1}(1 - e^{-kt})}, \tag{7}$$

where n_0 is the initial singlet exciton concentration, and k, the singlet exciton decay rate. A fit by Eq. (7) at short times ($<$40 ps) gives $\beta = 1.5 \times 10^{-9}$ cm^3/s for both the 75 and 420 μJ/cm^2 kinetics. The effective singlet exciton annihilation rate β is polymer specific and varies from 10^{-9} to 5×10^{-8} for different conjugated polymers.[12,13,22,23] The initial exciton concentration created by the laser pulse has a linear dependence on intensity up to 0.5 mJ/cm^2, showing that the 75 and 420 μJ/cm^2 light intensities are far from saturation [dashed line in Fig. 7(b)]. The normalized total photoluminescence (dotted line and circles) and the charge pair signal (solid line and triangles) are shown in Fig. 7(b) as well. The nonlinear intensity dependence of charge pair concentration shows that direct photogeneration of charge pairs (i.e., direct optical excitation of charge pairs) cannot be the main mechanism of charge pair generation in POMeOPT, because in that case the number of formed charge pairs should be proportional to the excitation intensity before saturation sets in. The leveling off of the intensity dependence of charge pair concentration in Fig. 7(b) cannot be explained by saturation of the optical transition since even the high intensity (420 μJ/cm^2) is far from absorption saturation. That we are far from saturation at these excitation intensities is also shown by the factor of 2 increase of charge concentration caused by the external electric field (see below). The same intensity dependence of charge pair concentration and total photoluminescence shown in Fig. 7(b), can be explained by exciton dissociation to charge pairs. Optical excitation at 2.5 eV creates singlet excitons that can migrate to another spectroscopic unit by hopping energy transfer, with characteristic hop times from sub-ps to picoseconds.[18] Increased excitation intensity leads to higher exciton concentration and probability for two excitons to meet on the same spectroscopic unit. When this happens, a spectroscopic unit may become doubly excited, and then very quickly it will return back to the lowest excited state by dissipating the excess energy as heat. The net result is that one exciton is quenched, annihilated. The annihilation process proceeds until there is only one exciton within the domain defined by the migration distance of the excitons and efficiently decreases the exciton concentration at high light intensities. We therefore attribute the nonlinear dependence of charge pair concentration on intensity, described by the data in Fig. 7, to exciton annihilation that opens up another channel for exciton quenching at high intensity.

Singlet exciton annihilation could in principle alter the rate and mechanism of charge pair formation, because high-energy excitons formed in the annihilation process have more excess energy to overcome a potential barrier.[10] We showed above that the light-induced charge pair formation is

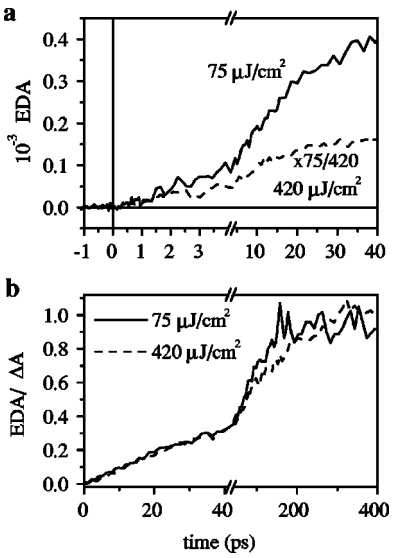

FIG. 8. (a) EDA dynamics at 1.55 eV after 75 μJ/cm^2 (solid line) and 420 μJ/cm^2 multiplied by a factor of 75/420 (dotted line) excitation. (b) EDA measured at 1.55 eV after 75 μJ/cm^2 (solid line) and 420 μJ/cm^2 (dashed line) excitation, divided by the corresponding ΔA dynamics.

low barrier or even barrierless in POMeOPT. Therefore it could be reasonable to assume that the excess energy supplied by the annihilation could lead to ultrafast hot exciton dissociation to charge pairs. To examine the exciton annihilation effect on charge pair formation, the EDA dynamics were normalized to the same number of initial excitons with 75 and 420 μJ/cm^2 (multiplied by a factor of 75/420) excitation intensity, monitored at 1.55 eV [Fig 8(a)]. The EDA dynamics at the two intensities overlap at early times (<2 ps), when annihilation does not decrease the number of excitons too much. At later times the normalized EDA kinetics at the higher intensity rises more slowly than the lower-intensity curve, as a result of exciton quenching caused by the annihilation [Fig. 8(a)]. Thus annihilation decreases the number of charge pairs, but from this representation of the data it is not clear whether this is a result of the decreased exciton concentration or decreased rate (probability) of charge pair formation. To receive information about that we normalize the two EDA curves to the number of excitons at each instant, by dividing the EDA kinetics with its corresponding ΔA kinetics [Fig. 8(b)]. From this we see that both curves coincide, showing that high-energy excitons formed in the annihilation process have the same probability to dissociate into charge pairs as vibrationally relaxed excitons. In other words, annihilation does not change the mechanism of charge pair formation in POMeOPT. The constant ratio of EDA/ΔA dynamics at long times [$\sim$1, in Fig. 8(b)] corresponds to approximately twice higher charge pair yield with $\sim$2 MV/cm external electric field, than without.

E. A model for charge pair generation

By comparison of the present results for POMeOPT with those previously obtained at similar experimental conditions for MeLPPP[9,10] we conclude that although the time scale and quantum yield of the charge pair generation from singlet excitons are similar for these two polymers there are nevertheless several differences in the charge pair formation mechanism:

(1) the exciton breaking in POMeOPT is a low-barrier process, while it is characterized by a substantial barrier in MeLPPP;

(2) in POMeOPT, as a result of the low-barrier exciton breaking, there is charge pair formation in the absence of an external electric field after excitation with light at low intensity and low photon energy. In MeLPPP charge pairs are only formed under different conditions—external electric field, high light intensity or high excitation photon energy;[8–11]

(3) singlet-singlet exciton annihilation speeds up charge pair generation in MeLPPP, while it leaves the rate essentially unchanged in POMeOPT;

(4) photoexcitation with $\sim$2 eV excess energy causes ultrafast dissociation of nonrelaxed excitons in MeLPPP.[10] in POMeOPT supplying comparable excess energy by annihilation does not exhibit detectable evidence of hot exciton dissociation.

These differences imply that the charge generation mechanism in POMeOPT is not the same as in MeLPPP. To account for this dissimilarity and also to explain the low yield of a nearly barrierless charge pair formation in POMeOPT we suggest two models of charge photogeneration—for MeLPPP type of behavior and for POMeOPT type. We start by giving a qualitative description of both cases and then we present a quantitative model for the low-barrier case, relevant to POMeOPT studied here. The corresponding account for the high-barrier case will be presented in a forthcoming publication.

The molecular approach of conjugated polymer photophysics assumes that the initially excited neutral singlet exciton breaks into a charge pair, which could be located at interchain or intrachain segments. The topology of the polymer film plays an important role in charge formation—we suggest that the exciton can dissociate at "special" dissociation sites, like chain crossings or aggregates (interchain dissociation), chain kinks, twists or other specific spectroscopic units (intrachain dissociation). These dissociation sites may have a much lower dissociation barrier as compared to all others sites. If on the other hand, the system is essentially homogeneous, i.e., there are no low-barrier dissociation sites, or the dissociation site density is low and excitation energy migration is slow, then charge generation occurs at random sites, if the energy barrier towards exciton breaking can be overcome. A simplified scheme of singlet exciton dissociation to charge pairs in a conjugated polymer is shown in Fig. 9(a) for a homogenous conjugated polymer and for a heterogeneous conjugated polymer containing dissociation sites [Fig. 9(b)]. In the homogenous (or the random site) model, light excitation creates singlet excitons, which undergo vibrational relaxation, internal conversion to ground state with rate k and dissociation to charges with rate γ. The overall apparent dissociation rate $\Gamma(t)$ is time dependent, as has been studied for MeLPPP.[9,10] This dependency is caused by higher probability to pass the energy barrier at higher excess energies and by the fact that different sites are characterized by different dissociation energy barriers, i.e., there is a dis-

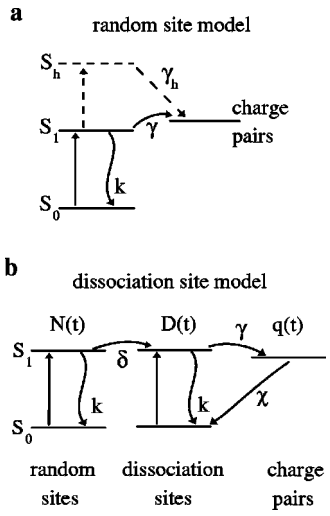

FIG. 9. Scheme of singlet exciton dissociation to charge pair in a homogenous (a) conjugated polymer (random site model) and for a heterogeneous conjugated polymer containing dissociation sites (b).

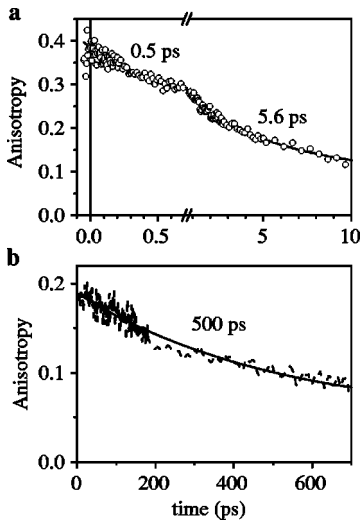

FIG. 10. Anisotropy dynamics of POMeOPT film (a) and POMeOPT in chloroform solution (b). Solid lines are exponential fits.

tribution of dissociation rates γ. Energy migration is not critical for exciton dissociation at random sites, because all sites are equal (within the distribution of the dissociation rate), while high energy excitation and singlet-singlet exciton annihilation can play an important role if the dissociaion energy barrier is high enough. In this case, a high excess energy exciton may form a charge pair with another rate γ_h, which can be several orders of magnitude higher than γ.[12,13]

In the alternative model, for a polymer with low-barrier dissociation sites, energy migration is crucial for charge generation at the dissociation sites, as a mechanism for excitons to reach those sites. Light excites both dissociation and nondissociation sites, but only excitons at dissociation sites can form charge pairs with the rate γ. In a low barrier case this rate is an effective dissociation rate that emerges from a competition of charge separation, geminate recombination and stabilization of separated charges by the external electric field and/or by interaction with phonons. The excitons at dissociation sites can also decay to the ground state with a rate k. A singlet exciton located at a nondissociation site can decay to the ground state with a rate k or migrate to neighboring sites, until it reaches a dissociation site. The rate of energy transfer to dissociation sites δ is not the site-to-site energy transfer rate, but represent several energy transfer steps. The time scale of this energy transfer is indicated by the anisotropy dynamics of POMeOPT film [Fig. 10(a)] and fluorescence anisotropy decay of POMeOPT in chloroform solution [Fig. 10(b)]. The initial anisotropy is approximately 0.4, showing that there is no sub-20-fs time component. A biexponential fit of the anisotropy dynamics in the polymer film gives the time constants 0.5 ± 0.2 ps and 5.6 ± 0.9 ps for fast energy migration.[18] It is important to realize that the anisotropy decay in the POMeOPT film (and in general an anisotropy decay) to zero is not the most representative measure of the total energy transfer time scale. The reason is that in film, with close-packed polymer chains, the energy transfer is faster than for the polymer in solution because of more available pathways. The anisotropy will therefore quickly decay to zero and becomes insensitive to further energy migration. The slow energy migration is represented by the anisotropy decay of POMeOPT in chloroform solution [Fig. 10(b)]. The decay is characterized by a 500 ps component representing energy transfer among isoenergetic polymer sites. This shows that the energy migration occurs during the entire lifetime of the exciton. In the dissociation site model for charge pair generation it is therefore reasonable to expect that this time scale will appear in the formation of charges. From the anisotropy measurements we thus see that energy migration in the polymer can be characterized by three time constants. In reality, there is a distribution of lifetimes due to the disordered nature of the polymer film. To simplify the modeling we will use fixed lifetimes for the energy transfer. It appears in addition that it is convenient to include the fast time scale (<10 ps) of energy transfer into the parameters describing charge generation at the special sites and direct optical excitation of the special sites (see below). The variable rate parameter for energy transfer then becomes characterized by a single rate $\delta<0.1$ ps^{-1}. Additional simplifications in the modeling are that we neglect energy transfer out from dissociation sites and charge recombination to excitons. After the presentation of the model we will comment on these simplifications. The data used in the modeling were collected at experimental conditions where singlet-singlet exciton annihilation only has a small contribution and is therefore neglected to simplify the analysis. With the energy level diagram of Fig. 9(b) we will now quantify the dissociation site model.

The total exciton concentration at each instant in time is a sum of the exciton concentration at dissociation sites, $D(t)$, the exciton concentration at nondissociation sites, which can reach dissociation sites, $N(t)$, and which never reach those sites, $n(t)$. The density of excitons at nondissociation sites, which can reach dissociation sites, is determined by the equation,

$$\begin{cases} \dfrac{dN(t)}{dt} = -kN(t) - \delta N(t), \\ N(t)|_{t=0} = N_0. \end{cases} \tag{8}$$

Solution of this equation gives a single-exponential decay,

$$N(t) = N_0 e^{-(k+\delta)t}. \tag{9}$$

The exciton concentration at dissociation sites can be found from the following kinetic equation,

$$\begin{cases} \dfrac{dD(t)}{dt} = \delta N(t) - kD(t) - \gamma D(t), \\ D(t)|_{t=0} = D_0, \end{cases} \tag{10}$$

as

$$D(t) = \left(D_0 - \frac{\delta N_0}{\gamma - \delta}\right) e^{-(k+\gamma)t} + \frac{\delta N_0}{\gamma - \delta} e^{-(k+\delta)t}, \tag{11}$$

where D_0 is the concentration of initially excited dissociation sites plus the concentration of excitons that reach dissociation sites during fast energy migration (<10 ps). The equation for the time evolution of the charge pair concentration is

$$\begin{cases} \dfrac{dq(t)}{dt} = \gamma D(t) - \chi q(t), \\ q(t)|_{t=0} = 0, \end{cases} \tag{12}$$

where χ is the charge pair decay rate. This equation can be solved as

$$q(t) = \frac{\gamma D_0 - \dfrac{\gamma \delta N_0}{\gamma - \delta}}{k + \gamma - \chi} (e^{-\chi t} - e^{-(k+\gamma)t}) + \frac{\dfrac{\gamma \delta N_0}{\gamma - \delta}}{k + \delta - \chi} (e^{-\chi t} - e^{-(k+\delta)t}). \tag{13}$$

Equation (13) has the same form as Eq. (3) with

$$B = \frac{\gamma D_0 - \dfrac{\gamma \delta N_0}{\gamma - \delta}}{k + \gamma - \chi}, \quad C = \frac{\dfrac{\gamma \delta N_0}{\gamma - \delta}}{k + \delta - \chi}, \quad t_1 = \frac{1}{\gamma + k},$$

$$t_2 = \frac{1}{\delta + k}, \quad t_3 = \frac{1}{\chi}.$$

An external electric field decreases the energy barrier for charge pair formation and slows down the immediate geminate recombination of charges by stabilization of separated charges, resulting in an increase of γ and in the appearance of additional dissociation sites. For simplicity we combine these effects in the effective increase of dissociation site concentration. The density of those new sites under 2 MV/cm external electric field is comparable with the dissociation site density in the absence of a field, because the charge pair yield is twice that without field (Fig. 8). A fit of the charge pair dynamics (Fig. 4), using Eq. (13), gives

$$\gamma = \frac{1}{10 \text{ ps}}, \quad \delta = \frac{1}{100 \text{ ps}}, \quad \frac{N_0}{D_0} = 2.8.$$

This means that on the average, for one directly excited singlet exciton at a dissociation site, or singlet exciton migrating to the dissociation site during fast energy transfer (<10 ps), there are three excitons created at nondissociation sites that can migrate to the dissociation sites during isoenergetic (slow) energy migration. There are still $n(t)|_{t=0} = n_0$ singlet excitons, that cannot reach dissociation sites, and their density can be found from the equation for the charge pair formation yield φ,

$$\varphi = \frac{\dfrac{\gamma}{k+\gamma}\left(D_0 + \dfrac{\delta}{k+\delta} N_0\right)}{D_0 + N_0 + n_0}. \tag{14}$$

Inserting the experimental charge pair formation yield $\varphi = 0.13$ into Eq. (14) gives the ratio $n_0/D_0 = 18$, implying that most excitons do not reach the dissociation sites during their lifetime. Using the fits of the EDA kinetics in Fig. 4 by formula (13) and using Eq. (14) we estimate the concentration of dissociation sites to 5% without external field, under the assumption that dissociation sites have the same absorption cross section as other sites. As mentioned above, this model contains several simplifications. A more detailed analysis including a distributed energy transfer rate to dissociation sites and consideration of energy migration from dissociation sites did not change the qualitative picture, but results in much more complicated fits with many free parameters, leading to ambiguity in the fitted parameters.

By comparing the experimental results of POMeOPT with MeLPPP we observe several qualitative differences in charge generation behavior (see above), which suggest that there are substantial differences in charge generation mechanism. We can now rationalize and understand the differences in charge pair generation of the two polymers, in terms of the model. The lack of influence on the charge generation rate and yield by high excess energy excitation in POMeOPT, as opposed to the ultrafast hot exciton dissociation in MeLPPP,[10] can be understood as a consequence of low dependence of the barrierless dissociation rate on excess energy and relatively slow energy transfer from random sites to dissociation sites. During the energy migration the excess energy supplied by a high energy photon or by exciton annihilation will be dissipated to the polymer heat bath and will not significantly influence the charge pair generation rate at a dissociation site.

In our dissociation site model, the conjugated polymer topology creates low barrier or even barrierless dissociation sites. These sites can be directly excited by light or can be reached during downhill and isoenergetic energy migration. It is only at dissociation sites where singlet excitons can form charge pairs. A similar approach has been used by Graupner *et al.* to explain charge photogeneration in MeLPPP.[8] These authors conclude that the major contribution to charge pair formation dynamics appears from the downhill energy migration. We conclude that our own measurements of charge pair photogeneration in MeLPPP[9] under

annihilation-free conditions of excitation with ~100 times weaker light intensity than in Ref. 8 fit well to the random site generation mechanism and cannot be explained by the "dissociation site" model. At high pump intensity excitation, energy migration in MeLPPP will lead to singlet-singlet annihilation resulting in formation of additional effective "special" sites with much higher dissociation rate.[10] Under these conditions, charge pair generation in MeLPPP will become sensitive to excitation energy migration as predicted by the "dissociation site" model, but we believe that a more appropriate description of the dynamics involves a "random site" model rather than a modified "dissociation site" model, since the application of a model is determined by the polymer film features (energetics, morphology, dynamics, etc.) and is receptive to the excitation conditions. We can conclude that the charge generation in POMeOPT can be well treated by the dissociation site model, while the random site model is more applicable for MeLPPP. These two models or a combination of them may be useful to address photoinduced charge generation in other conjugated polymers.

IV. CONCLUSIONS

The results of the above discussion can be summarized as follows:

(1) Charge pair formation in POMeOPT occurs from breaking of singlet excitons at low-barrier dissociation sites. The estimated density of those sites is ~5%, and there are two mechanisms to reach the dissociation site—direct optical excitation and energy migration.

(2) Due to the low-barrier exciton dissociation in POMeOPT, there is charge pair formation in the absence of an external electric field and the number of formed charge pairs has a parabolic electric field dependence.

(3) The charge pair formation yield in POMeOPT is ~13% without external field and ~26% with 2 MV/cm external electric field.

(4) Supplying 1.1 eV excess energy by high energy photon excitation or ~2.0 eV excess energy by exciton annihilation does not exhibit detectable evidence of hot exciton dissociation in POMeOPT, because of possible weak dependence of the barrierless dissociation rate on excess energy and fast dissipation of the excess energy during exciton migration towards dissociation sites.

ACKNOWLEDGMENTS

We are indebted to Mattias Svensson and Mats Andersson from Chalmers University of Technology (Sweden) for providing POMeOPT and Wichard Beenken from Lund University (Sweden) for useful discussions. We acknowledge the Knut and Allice Wallenberg foundation, the Swedish Institute, the Crafoord Foundation and the EU-TMR program (HPRI-CT-1999-00041) for financial support.

*Electronic address: Arkady.Yartsev@chemphys.lu.se

[1] D. Moses, A. Dogariu, and A. J. Heeger, Phys. Rev. B **61**, 9373 (2000).
[2] D. Moses, A. Dogariu, and A. J. Heeger, Synth. Met. **116**, 19 (2001).
[3] R. Kersting, U. Lemmer, M. Deussen, H. J. Bakker, R. F. Mahrt, H. Kurz, V. I. Arkhipov, H. Bässler, and E. O. Göbel, Phys. Rev. Lett. **73**, 1440 (1994).
[4] S. Barth and H. Bässler, Phys. Rev. Lett. **79**, 4445 (1997).
[5] S. Barth, H. Bässler, U. Scherf, and K. Müllen, Chem. Phys. Lett. **288**, 147 (1998).
[6] V. I. Arkhipov, E. V. Emelianova, and H. Bässler, Phys. Rev. Lett. **82**, 1321 (1999).
[7] V. I. Arkhipov, E. V. Emelianova, S. Barth, and H. Bässler, Phys. Rev. B **61**, 8207 (2000).
[8] W. Graupner, G. Cerullo, G. Lanzani, M. Nisoli, E. J. W. List, G. Leising, and S. De Silvestri, Phys. Rev. Lett. **81**, 3259 (1998).
[9] V. Gulbinas, Y. Zaushitsyn, V. Sundström, D. Hertel, H. Bässler, and A. Yartsev, Phys. Rev. Lett. **89**, 107401 (2002).
[10] V. Gulbinas, Y. Zaushitsyn, H. Bässler, A. Yartsev, and V. Sundström (unpublished).
[11] J. G. Muller, U. Lemmer, J. Feldmann, and U. Scherf, Phys. Rev. Lett. **88**, 147401 (2002).
[12] C. Silva, A. S. Dhoot, D. M. Russell, M. A. Stevens, A. C. Arias, J. D. MacKenzie, N. C. Greenham, R. H. Friend, S. Setayesh, and K. Mullen, Phys. Rev. B **64**, 125211 (2001).
[13] G. Denton, N. Tessler, M. Stevens, and R. H. Friend, Synth. Met. **102**, 1008 (1999).
[14] A. Ruseckas, M. Theander, M. R. Andersson, M. Svensson, M. Prato, I. Inganäs, and V. Sundström, Chem. Phys. Lett. **322**, 136 (2000).
[15] S. V. Frolov, X. Wei, W. Gellermann, Z. Vardeny, and E. Ehrenfreund, Chem. Phys. **227**, 125 (1998).
[16] X. Wei, Z. V. Vardeny, N. S. Sariciftci, and A. J. Heeger, Phys. Rev. B **53**, 2187 (1996).
[17] M. Svensson, M. Theander, O. Inganas, and M. Andersson, Synth. Met. **119**, 113 (2001).
[18] Mette M. L. Grage, Y. Zaushitsyn, A. Yartsev, M. Chachisvilis, V. Sundström, and T. Pullerits, Phys. Rev. B **67**, 205207 (2003).
[19] D. Zigmantas, T. Polivka, R. Hiller, A. Yartsev, and V. Sundström, J. Phys. Chem. A **105**, 10296 (2001).
[20] V. Gulbinas, R. Kananavicius, L. Valkunas, and H. Bässler, Phys. Rev. B **66**, 233203 (2002).
[21] M. Hilczer, S. Traytak, and M. Tachiya, J. Chem. Phys. **115**, 11249 (2002).
[22] Y. Zaushitsyn, K. Jespersen, V. Sundström, and A. Yartsev (unpublished).
[23] M. Stevens, C. Silva, D. Russell, and R. H. Friend, Phys. Rev. B **63**, 165213 (2001).